

Quantitative Optical Coherence Tomography Detection of New Neovascular Branches and Association With Exudation Recurrence in Neovascular Age-Related Macular Degeneration

Alessandro Arrigo,^{1,2} Emanuela Aragona,¹ Sebastiano Del Fabbro,¹ Edoardo Balduzzi,¹ Maurizio Battaglia Parodi,¹ and Francesco Bandello¹

¹Ophthalmology Unit, IRCCS San Raffaele Scientific Institute, Milan, Italy

²Eye Repair Unit, Division of Neuroscience, IRCCS San Raffaele Scientific Institute, Milan, Italy

Correspondence: Alessandro Arrigo, Department of Ophthalmology, IRCCS San Raffaele Scientific Institute, via Olgettina 60, Milan 20132, Italy; alessandro.arrigo@hotmail.com.

Received: March 17, 2024

Accepted: June 3, 2024

Published: June 20, 2024

Citation: Arrigo A, Aragona E, Del Fabbro S, Balduzzi E, Parodi MB, Bandello F. Quantitative optical coherence tomography detection of new neovascular branches and association with exudation recurrence in neovascular age-related macular degeneration. *Invest Ophthalmol Vis Sci.* 2024;65(6):30. <https://doi.org/10.1167/iovs.65.6.30>

PURPOSE. The purpose of this study was to investigate the clinical role of multi-signal quantitative optical coherence tomography angiography (OCTA) perfusion sampling in neovascular age-related macular degeneration (AMD).

METHODS. The study was designed as a cross-sectional case series. We collected data from already treated macular neovascularization (MNV), characterized by (I) clinically relevant recurrent exudation, (II) nonclinically relevant recurrent exudation, and (III) inactive lesion. We proposed a new OCTA metric, calculating the gap between high-resolution (HR) and high-speed (HS) OCTA samplings, hypothesizing that this gap might improve the detection of new secondary MNV branches, being also associated with exudation recurrence. Main outcome measures were the HR-HS gap-based categorization of MNV lesions and the assessment of its association with exudative, minimally exudative, and inactive lesions.

RESULTS. Our cohort (which consisted of 32 MNV eyes; 32 patients; mean disease duration 5 years) was classified as type 1 (17; 53%), type 2 (11; 34%), or mixed type (4; 13%) MNV. Subretinal fibrosis was found in 17 out of 32 eyes (53%), whereas outer retinal atrophy involved 22 of 32 eyes (69%). HR-HS MNV gap was significantly different among MNV subgroups: 18% for the exudative subgroup, 12% for the minimally exudative subgroup, and 4% for the inactive subgroup. HR-HS gap significantly correlated with best corrected visual acuity (BCVA), disease duration, fibrosis, and outer retinal atrophy.

CONCLUSIONS. HR-HS gap is a novel quantitative metric to detect the secondary novel branches of AMD-related MNV. This parameter is clinically relevant because it is associated with fluid recurrence. The integration of HR-HS gap in artificial intelligence models might help to predict MNV reactivation and to optimize treatment strategies.

Keywords: neovascular age-related macular degeneration (AMD), macular neovascularization (MNV), optical coherence tomography (OCT), optical coherence tomography angiography (OCTA), exudation, high resolution – high speed (HR-HS) gap

Macular neovascularization (MNV) is a complication occurring in at least 20% to 30% of patients with age-related macular degeneration (AMD).¹ Multimodal retinal imaging, including optical coherence tomography (OCT) and OCT angiography (OCTA), provided a powerful set of tools allowing the noninvasive, in vivo assessment of neovascular AMD characteristics.^{2–7} The adoption of even advanced quantitative approaches is providing much more detail regarding the relationship between MNV perfusion features and clinical outcomes.^{4–6} The quantitative evaluation of MNV morphology has also proved useful in assessing the factors associated with different responses to anti-VEGF treatments as well as different progression rates.^{7–10} Up to now, OCTA data could be collected only by using fixed acquisition parameters. However, some OCTA devices can now

allow the customization of acquisition metrics, thus potentially allowing the sampling of different types of perfusion signal. In a recent study, we showed how the combined use of high-resolution (HR) and high-speed (HS) OCTA acquisitions allowed to improve the perfusion signal sampling in healthy subjects.¹¹ On this basis, the main hypothesis of the present study is that HR-HS gap evaluation might be useful to distinguish exudative from nonexudative MNV lesions in neovascular AMD.

MATERIALS AND METHODS

The study was designed as an observational, cross-sectional study. All the patients were recruited at the Ophthalmology Unit of IRCCS San Raffaele Scientific Institute, Milan,



Italy. We obtained a signed informed consent from all the patients before their inclusion in the study. The study was approved by the local Ethical Committee (MIRD2020). The entire research was conducted in accordance with the Declaration of Helsinki. The inclusion criterion was the diagnosis of AMD, complicated by type 1, type 2, or mixed type 1/2 MNV lesions already under treatment. We included only one eye for each patient. In case of bilaterality, we chose the eye with the best quality of the images. Otherwise, we arbitrarily selected the right eye. We excluded type 3 and aneurysmal type 1 lesions because of them being associated with low quality of the images. Moreover, we excluded newly diagnosed lesions, because the main study goal was to detect MNV lesions characterized by fluid recurrence from inactive lesions. Further exclusion criteria were high media opacities, any ocular surgery performed in the 6 months before the inclusion in the study, other ocular disorders (for example, glaucoma or uveitis), and uncontrolled system conditions potentially interfering with the proper interpretation of the results. All the patients are treated by means of intravitreal anti-VEGF injections in a real-life setting, accordingly with ophthalmologists' discretion.

Because all the MNVs were already treated, we used clinical records to trace the original diagnosis of type 1, mixed, or type 2 lesion.

Ophthalmologic examination included logMAR best corrected visual acuity (BCVA), measured using standard Early Treatment Diabetic Retinopathy Study (ETDRS) charts, slit lamp biomicroscopy, and Goldmann applanation tonometry. The structural OCT (Spectralis HRA+OCT; Heidelberg Engineering, Heidelberg, Germany) acquisition protocol included raster, radial, and dense scans, with a high number of frames (ART > 25) and enhanced depth imaging (EDI). OCT scans were used to assess the presence of fluid recurrence. We separately considered subretinal fluid (SRF), intraretinal fluid (IRF), subretinal hyper-reflective material (SHRM), and pigment epithelium detachment (PED). Because of being associated with poor image quality, we excluded those cases characterized by PED height > 200 μm . Based on similar criteria adopted in the FLUID study,¹² an expert grader (author S.D.L.) classified the eyes in three subgroups: (I) clinically relevant fluid recurrence (any IRF or SHRM; SRF > 200 μm ; the exudative group); (II) not clinically relevant fluid recurrence (SRF < 200 μm ; the minimally exudative group); and (III) inactive lesion (any sign of fluid; the dry group).

The OCTA acquisition protocol included HR OCTA scan (OCT scan angle 10 degrees, lateral pixel spacing approximately 5.73 $\mu\text{m}/\text{pixels}$, digital depth resolution 3.87 $\mu\text{m}/\text{pixels}$, ART 7 images, 512 B-scans, and inter B-scan distance 12 μm) and HS OCTA scan (scan angle 10 degrees, lateral pixel spacing approximately 11.46 $\mu\text{m}/\text{pixels}$, ART 7 images, number of images 256, and inter B-scans distance 12 μm). From OCTA reconstructions, we extracted the automatic segmentations of the superficial capillary plexus (SCP), deep capillary plexus (DCP), choriocapillaris (CC), and MNV network, performed by the on-board software. Each segmentation was carefully inspected by an expert grader (author S.D.L.) and manually corrected to assess the vertical extension of the MNV. From the same OCTA acquisitions, we exported the enface OCT reconstruction, including the recurrent fluid in its entirety. By this way, the fluid could be visually inspected as a hyporeflective signal in the enface OCT. Only high-quality images (HEYEX score > 25) were included into the analyses.

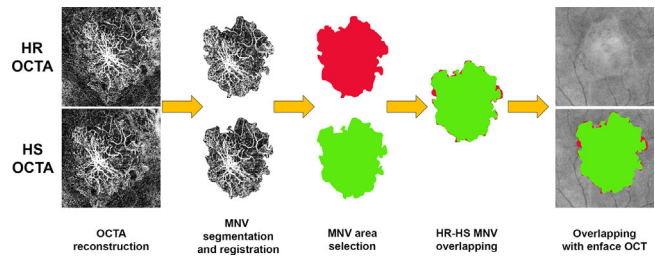


FIGURE 1. Pipeline for HR-HS MNV gap calculation. Starting from HR OCTA and HS OCTA, MNV reconstructions are segmented, isolated and coregistered. The MNV area is colored and the two MNV areas are overlapped. The resulting image is overlapped on the enface OCT reconstruction. The HR-HS MNV gap is highlighted by the exceeding red borders. Enface OCT is used to evaluate spatial agreement with exudation recurrence.

MNV segmentations were obtained by using the same coordinates and were not manually adjusted or altered to not interfere with the proper calculation of the quantitative metrics. Both for HR and HS OCTA acquisitions, the same unblinded expert grader (author S.D.L.) carefully selected only the neovascular network, removing all the background signal, including spurious particle motion signal and residual of retinal capillaries or CC, and automatically selecting the borders of the remaining image (the MNV network alone) through a region-finder tool provided in ImageJ.¹³

As a preliminary step, all the MNV reconstructions were set to the same grayscale range to address possible confounding factors related with the quality of the images and the intensity of the signal. The background was set to absolute black to avoid possible issues related with different contrast to noise ratio. A blinded grader (author E.B.) used the following pipeline, based on ImageJ scripts, to analyze MNV network, considering both HR and HS OCTA acquisitions: HR and HS MNV registration -> MNV boundaries selection -> delineation of HR and HS MNV area -> overlapping of HR and HS MNV area -> calculation of HR/HS MNV area gap. The entire pipeline is visually shown in Figure 1. The entire pipeline was repeated at least twice by the same grader to test repeatability (resulting as > 95% of agreement; range = 0.96-1.00). By this way, we assumed that HR/HS MNV area gap may be a measure of the secondary novel branches of the MNV network. These are intended as the peripheral immature capillaries characterized by lower perfusion with respect to the central core of the MNV, representing the front of growth of the MNV lesion, and potentially causing exudation recurrence.

Both graders were involved to qualitatively test the spatial relationship between the HR and HS MNV areas and the fluid area, when present. The overlapped HR and HS MNV area reconstructions were superimposed on the enface OCT highlighting fluid. The graders evaluated the agreement between the HR-HS MNV gap area and the fluid area. In particular, the graders selected only the fluid area on enface OCT and the HR-HS MNV gap area. Then, they calculated the overlapping factor considering the common pixels of both areas, categorized as follows: (I) optimal agreement (> 80% of overlapping fraction), (II) partial agreement (50-80% of overlapping fraction), and (III) poor agreement (< 50% of overlapping fraction).

The statistical analyses included age and gender as fixed factors. We also included the following variables: total

number of intravitreal anti-VEGF injections administered, duration of the disease (because the onset of neovascular AMD), subretinal fibrosis (defined as the presence of subretinal or subretinal pigment epithelium hyper-reflective lesion with multilaminar appearance) and outer retinal atrophy (defined as the loss of the ellipsoid and interdigitation zones associated with thinning of the outer nuclear layer, with or without decreased or absent retinal pigment epithelium and choroidal hypertransmission).¹⁴ We tested the distribution normality for each variable by frequency histograms and quantile-quantile plots. Continuous variables were reported as mean \pm standard deviation, whereas frequency and proportions were reported as categorical variables. Two-tailed *t* test was used to analyze continuous variables. Mixed models were used to assess the relationships among the collected variables. We considered three subgroups: (I) clinically relevant fluid recurrence; (II) not clinically relevant fluid recurrence; and (III) inactive lesion. Bonferroni correction for multiple comparisons was used when needed. One-way ANOVA analysis was used to test inter-group differences in terms of fibrosis and atrophy prevalence weighted for disease duration. Interclass correlation coefficient (ICC) was calculated for those metrics collected by both graders. We set statistical significance to *P* value \leq 0.05.

RESULTS

Our study involved 32 MNV eyes of 32 patients with AMD (15 male patients; mean age = 74 ± 5 years). The mean HEYEX quality score was 29 (range = 25–34). Mean BCVA was 0.5 ± 0.2 logMAR (range = 0.1–0.9). The mean disease duration was 5 years (range = 3–8 years). The mean number of intravitreal injections was 20 (range = 10–31).

Based on clinical records, MNV were classified as type 1 (17; 53%), type 2 (11; 34%) or mixed type (4; 13%). Subretinal fibrosis was found in 17 of 32 eyes (53%), whereas outer retinal atrophy interested 22 of 32 eyes (69%).

Overall, the MNV area resulted 1.54 ± 0.41 for HR OCTA and 1.34 ± 0.42 for HS OCTA ($P < 0.001$). In all the cases, HR OCTA detected a bigger MNV area than HS OCTA. Considering the subgroup analysis, the exudative subgroup and the minimally exudative subgroup showed similar MNV area for HR OCTA (1.43 ± 0.37 vs. 1.45 ± 0.39 , respectively; $P > 0.05$) and HS OCTA (1.17 ± 0.31 vs. 1.28 ± 0.35 , respectively; $P > 0.05$). Conversely, the dry subgroup showed a significantly bigger MNV area than the other two subgroups, both considering HR OCTA (1.85 ± 0.38 ; $P < 0.001$) and HS OCTA (1.79 ± 0.39 ; $P < 0.001$). HR-HS MNV gap was significantly different among the 3 subgroups: 18% for the exudative subgroup, 12% for the minimally exudative subgroup, and 4% for the dry subgroup ($P < 0.001$). Example cases are shown in Figures 2–4. The HR-HS MNV gap showed high agreement with the area of fluid. In the exudative subgroup, the fluid area exceeded the HR-HS MNV gap area, resulting in a bigger area in 100% of the cases. The overlapping fraction was optimal in the entire exudative subgroup (mean = 92.5%, range = 85–99%; $P < 0.001$; ICC = 0.96; range = 0.94–0.99; $P < 0.001$). In the minimally exudative subgroup, the HR-HS MNV gap showed good agreement with the area of fluid. In this subgroup, the fluid area showed higher variability in terms of localization, with overlapping fraction resulting overall partial in the entire minimally exudative subgroup (mean = 67.7%; range = 56–89%; $P < 0.001$; ICC = 0.91; range = 0.87–0.94; $P < 0.001$).

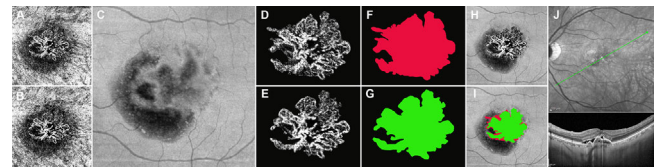


FIGURE 2. The HR-HS MNV gap in exudative MNV. HR OCTA (A) and HS OCTA (B) well detected the MNV network. Enface OCT (C) confirmed the presence of fluid (black areas). MNV reconstructions (D, E) are isolated, coregistered, and colored in red (HR OCTA) (F) and green (HS OCTA) (G), respectively. Then, the overlapped areas are superimposed on enface OCT (H, I). In this case, the HR-HS MNV gap resulted in $> 18\%$, with high agreement between HR-HS MNV gap area and fluid area localization. Structural OCT (J) confirmed the presence of fluid recurrence.

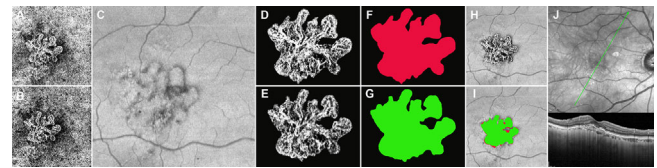


FIGURE 3. The HR-HS MNV gap in minimally exudative MNV. HR OCTA (A) and HS OCTA (B) well detected the MNV. Enface OCT (C) confirmed the presence of small areas of fluid (black areas). MNV reconstructions (D, E) are isolated, coregistered, and colored in red (HR OCTA) (F) and green (HS OCTA) (G), respectively. Then, the overlapped areas are superimposed on enface OCT (H, I). In this case, the HR-HS MNV gap resulted $< 15\%$, with high agreement between the HR-HS MNV gap area and the fluid area localization. Structural OCT (J) confirmed the presence of subclinical fluid recurrence ($< 200 \mu\text{m}$ of subretinal fluid and no intraretinal fluid).

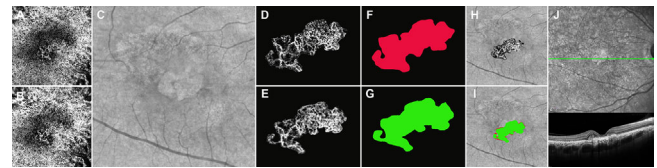


FIGURE 4. HR-HS MNV gap in inactive MNV. HR OCTA (A) and HS OCTA (B) well detected the MNV. Enface OCT (C) confirmed the absence of (no black areas). MNV reconstructions (D, E) are isolated, coregistered, and colored in red (HR OCTA) (F) and green (HS OCTA) (G), respectively. Then, the overlapped areas are superimposed on enface OCT (H, I). In this case, the HR-HS MNV gap resulted in $< 10\%$. Structural OCT (J) confirmed the absence of fluid.

Similarly, the logMAR BCVA significantly differed among the subgroups, being the worst in the dry subgroup ($P < 0.001$). Disease duration and total number of injections was quite higher in the dry subgroup than in the other subgroups. Moreover, we found statistically significant differences among the exudative subgroup, the minimally exudative subgroup, and the dry subgroup in terms of prevalence of fibrosis (28%, 67%, and 100%, respectively; $P < 0.001$) and outer retinal atrophy (50%, 83%, and 100%, respectively; $P < 0.001$). The entire subgroups analysis is shown in the Table.

The correlation analysis highlighted statistically significant correlations for logMAR BCVA considering disease duration (Tau-Kendall coefficient = 0.537; $P < 0.001$), MNV subgroups (Tau-Kendall coefficient = 0.523; $P < 0.001$), fibrosis (Tau-Kendall coefficient = 0.707; $P < 0.001$), and outer retinal atrophy (Tau-Kendall coefficient = 0.684; $P < 0.001$). Moreover, the HR-HS MNV gap significantly corre-

TABLE. MNV Subgroups Analysis

	MNV Subgroups Analysis		
	Exudative Subgroup	Minimally Exudative Subgroup	Dry Subgroup
Group	1	2	3
N of eyes	18	6	8
Age, y	79 ± 5	82 ± 5	81 ± 3
Disease duration, y	4 ± 1	6 ± 2	7 ± 2
LogMAR BCVA	0.39 ± 0.19	0.52 ± 0.16	0.74 ± 0.16
Total number of intravitreal injections	17 ± 5	22 ± 6	24 ± 6
MNV area HR OCTA, mm ²	1.43 ± 0.37	1.45 ± 0.39	1.85 ± 0.38
MNV area HS OCTA, mm ²	1.17 ± 0.31	1.28 ± 0.35	1.79 ± 0.39
HR-HS gap, (%)	18 ± 2	12 ± 1	4 ± 3
Fibrosis	5/18 (28%)	4/6 (67%)	8/8 (100%)
Outer retinal atrophy	9/18 (50%)	5/6 (83%)	8/8 (100%)
	P Value		
	1 vs. 2	1 vs. 3	2 vs. 3
Age, y	>0.05	>0.05	>0.05
Disease duration, y	=0.02	=0.003	>0.05
LogMAR BCVA	>0.05	<0.001	<0.001
Total number of intravitreal injections	>0.05	=0.012	>0.05
MNV area HR OCTA	>0.05	=0.03	>0.05
MNV area HS OCTA	>0.05	<0.001	=0.03
HR-HS gap	<0.001	<0.001	<0.001
Fibrosis	<0.001	<0.001	<0.001
Outer retinal atrophy	<0.001	<0.001	<0.001

lated with logMAR BCVA (Tau-Kendall coefficient = -0.390; *P* = 0.003), disease duration (Tau-Kendall coefficient = -0.396; *P* = 0.003), fibrosis (Tau-Kendall coefficient = -0.515; *P* < 0.001), and outer retinal atrophy (Tau-Kendall coefficient = -0.351; *P* = 0.01). In addition, MNV type (type 1, type 2, or mixed 1/2 type) significantly correlated with logMAR BCVA (Tau-Kendall coefficient = 0.472; *P* = 0.002), outer retinal atrophy (Tau-Kendall coefficient = 0.367; *P* = 0.03), HR OCTA MNV area (Tau-Kendall coefficient = 0.470; *P* < 0.001), and HS OCTA MNV area (Tau-Kendall coefficient = 0.506; *P* < 0.001).

DISCUSSION

In the present study, we described a new potential metric associated with fluid recurrence in neovascular AMD, named the HR-HS MNV gap. This represents the percentage difference between two OCTA acquisitions obtained by using different acquisition metrics. In particular, HR OCTA is characterized by higher resolution and longer acquisition time, whereas HS OCTA can be obtained faster, although reducing the resolution of the images. Actually, the agreement between HR and HS OCTA acquisitions for detecting MNV was very high, differing for a maximum of 18% in the exudative subgroup. This finding was in line with previous investigations supporting the feasibility of both acquisitions.^{11,12,14,15} However, the oversampling provided by HR OCTA allowed to detect much more details regarding the peripheral parts of the MNV, where the new branches usually grew, with respect to the central and more mature part of the neovascular network.¹² Indeed, the central core of the MNV is usually characterized by high perfusion signal (high reflectivity), whereas it centrifugally decreases reaching the peripheral areas.⁹ Whereas the core undergoes to vascular maturity and stabilization of growth, the peripheral part may be interested by size expansion over time.¹⁰

On this basis, the analysis of the peripheral perfusion signal may be used to predict the MNV expansion, caused by the growth of new neovascular capillaries.¹⁰ On this basis, the HR-HS MNV gap might be considered a measure of this growth, resulting bigger in those eyes characterized by fluid recurrence, and minimal in eyes with inactive MNV lesions. The HR/HS gap-based analysis of the growth front of the MNV network is supported by a previous OCTA investigation showing that high percentages of branching with tiny vessels and of peripheral arcades at the borders of the MNV were significantly associated with higher risk of exudation recurrence.^{16,17} In particular, in this study, we separately analyzed eyes characterized by clinically relevant fluid recurrence, nonclinically relevant fluid recurrence, and inactive MNV. The HR-HS MNV gap significantly differed among these subgroups, being the biggest in the exudative subgroup and the lowest in the dry subgroup. This latter subgroup was also characterized by higher disease duration, higher number of intravitreal injections, bigger MNV area, and higher prevalence of fibrosis and atrophy, thus indicating older and more advanced MNV lesions. At the same time, the significantly higher prevalence of fibrosis and atrophy in the minimally exudative subgroup, with respect to the exudative subgroup, indicated more mature lesions, although still characterized by mild exudative phenomena.

The high agreement between the HR-HS MNV gap area and the fluid area might be explained considering the vascular remodeling occurring in MNV over time. Indeed, while the original neovascular network matures, it is possible to observe changes in network angiographic features, with thickening of the neovascular capillaries probably caused by sclerotizing phenomena.^{18,19} Conversely, novel branches are thinner and closely interconnected.^{18,19} On this basis, we may hypothesize that the sclerotization of the MNV core leads to the stabilization of the blood-retinal barrier, thus limiting further exudative phenomena. On the contrary, the

novel branches are characterized by completely disrupted blood-retinal barrier, thus causing exudation recurrence. The exudation area resulted bigger than HR-HS MNV gap area because the fluid can expand within the retinal structures and the subretinal space. This hypothesis is supported by the evidence that peripheral loop detections are associated with recurrent exudation.²⁰ However, the cited study is limited by the fact that the presence of peripheral MNV loops was qualitatively assessed. The quantitative approach based on HR-HS MNV gap calculation allows a highly reproducible and objective way to study peripheral changes of the neovascular network. In addition, it might be implemented in artificial intelligence tools to improve disease monitoring and recurrence prediction.

The HR-HS MNV gap had a clinical relevance, showing significant inverse correlations with disease duration, fibrosis, and outer retinal atrophy, suggesting that the higher is the HR-HS MNV gap, the younger (and more active) is the MNV. This finding is supported by the evidence that MNV activity decreases over the years, if adequately managed by anti-VEGF injections.^{21,22}

We are aware that our study labors under several limitations, first related to the small number of eyes and the cross-sectional design. We have not repeated HR and HS OCTA acquisitions to not cause excessive distress for the patients, leading to the risk of poor-quality data. However, we could not provide objective data regarding the repeatability of MNV network detection by the two different acquisitions. However, we may confirm that the expert grader easily detected the MNV network both with HR and HS OCTA scans in all the included eyes. The lack of prospective data about the role of the HR-HS MNV gap in predicting fluid recurrence should be adequately addressed by future prospective study. In addition, we did not assess the contribution of subretinal and intraretinal fluids separately. It is known that the origin of subretinal and intraretinal fluids is different, with the first one more associated with the neovascular activity and the second one more associated with inner blood-retinal barrier impairment.²³ Because of the importance of the separate assessment of each type of fluids, future studies should be focused on testing their relationship with the proposed HR-HS MNV gap metric. Considering all these points, this should be considered only a feasibility investigation regarding the use of HR-HS MNV gap in clinical practice. The high technical skills required by the graders and the time-consuming analyses represents another potential limitation, which could be solved by developing automatic tools or integrating this method in artificial intelligence algorithms. Most of the proposed methodologies are novel and cutoffs arbitrarily established, thus requiring future support and validation. In addition, the need of two consecutive OCTA acquisitions might be time-consuming in clinical practice and potentially distressful for the patients. However, the improvements in OCTA devices speed and eye-tracking performance still allow the feasible collection of the required data also in a real clinical setting. Moreover, OCTA techniques are well known to be potentially artifact prone.²⁴

In conclusion, our study proposed a novel quantitative approach to evaluate the novel branches in neovascular AMD. Their detection is significantly associated with exudation recurrence. The HR-HS MNV gap is potentially clinically useful, being associated with MNV activity, disease duration, fibro-atrophic evolution, and visual outcome. Its use in automatic tools and in artificial intelligence algorithms might improve the customization of patients' diag-

nostic workup and treatment strategies. Further prospective studies are needed to confirm and support our findings.

Acknowledgments

Disclosure: **A. Arrigo**, None; **E. Aragona**, None; **S. Del Fabbro**, None; **E. Balduzzi**, None; **M.B. Parodi**, None; **F. Bandello**, Alcon (Fort Worth, TX, USA) (C), Alimera Sciences (Alpharetta, GA, USA) (C), AbbVie Inc. (North Chicago, IL, USA) (C), Farmila-Thea (Clermont-Ferrand, France) (C), Bayer Shering-Pharma (Berlin, Germany) (C), Bausch and Lomb (Rochester, NY, USA) (C), Genentech (San Francisco, CA, USA) (C), Hoffmann-La-Roche (Basel, Switzerland) (C), NovagaliPharma (Évry, France) (C), Novartis (Basel, Switzerland) (C), Sanofi-Aventis (Paris, France) (C), Thrombogenics (Heverlee, Belgium) (C), Zeiss (Dublin, CA, USA) (C)

References

1. Wong TY, Chakravarthy U, Klein R, et al. The natural history and prognosis of neovascular age-related macular degeneration: a systematic review of the literature and meta-analysis. *Ophthalmology*. 2008;115(1):116–126.
2. Farecki ML, Gutfleisch M, Faatz H, et al. Characteristics of type 1 and 2 CNV in exudative AMD in OCT-angiography. *Graefes Arch Clin Exp Ophthalmol*. 2017;255(5):913–921.
3. Arrigo A, Aragona E, Capone L, et al. Advanced optical coherence tomography angiography analysis of age-related macular degeneration complicated by onset of unilateral choroidal neovascularization. *Am J Ophthalmol*. 2018;195:233–242.
4. Arrigo A, Romano F, Aragona E, et al. Optical coherence tomography angiography can categorize different subgroups of choroidal neovascularization secondary to age-related macular degeneration. *Retina*. 2020;40(12):2263–2269.
5. Arrigo A, Aragona E, Di Nunzio C, Bandello F, Parodi MB. Quantitative optical coherence tomography angiography parameters in type 1 macular neovascularization secondary to age-related macular degeneration. *Transl Vis Sci Technol*. 2020;9(9):48.
6. Arrigo A, Bordato A, Aragona E, et al. Macular neovascularization in AMD, CSC and best vitelliform macular dystrophy: quantitative OCTA detects distinct clinical entities. *Eye (Lond)*. 2021;35(12):3266–3276.
7. Uchida A, Hu M, Babiuch A, et al. Optical coherence tomography angiography characteristics of choroidal neovascularization requiring varied dosing frequencies in treat-and-extend management: an analysis of the AVATAR study. *PLoS One*. 2019;14(6):e0218889.
8. Arrigo A, Aragona E, Bordato A, et al. Quantitative optical coherence tomography angiography parameter variations after treatment of macular neovascularization secondary to age-related macular degeneration. *Retina*. 2021;41(7):1463–1469.
9. Arrigo A, Aragona E, Bordato A, et al. High reflectivity and low reflectivity properties on OCTA influence the detection of macular neovascularization in AMD. *Front Phys*. 2021;9:353.
10. Arrigo A, Amato A, Mularoni C, et al. Optical coherence tomography angiography parameters correlated to the growth of macular neovascularization in age-related macular degeneration. *Front Phys*. 2022;10:2022.
11. Arrigo A, Teussink M, Bianco L, et al. High-resolution/high-speed gap can distinguish different intraretinal perfusion signals by optical coherence tomography angiography. *Transl Vis Sci Technol*. 2023;12(5):11.
12. Guymer RH, Markey CM, McAllister IL, et al. Tolerating subretinal fluid in neovascular age-related macular degen-

- eration treated with ranibizumab using a treat-and-extend regimen: FLUID study 24-month results. *Ophthalmology*. 2019;126(5):723–734.
13. Schindelin J, Arganda-Carreras I, Frise E, et al. Fiji: an open-source platform for biological-image analysis. *Nat Methods*. 2012;9(7):676–682.
 14. Spaide RF, Jaffe GJ, Sarraf D, et al. Consensus nomenclature for reporting neovascular age-related macular degeneration data: consensus on neovascular age-related macular degeneration nomenclature study group. *Ophthalmology*. 2020;127(5):616–636.
 15. Corvi F, Corradetti G, Parrulli S, et al. Comparison and repeatability of high resolution and high speed scans from spectralis optical coherence tomography angiography. *Transl Vis Sci Technol*. 2020;9(10):29.
 16. Nakano Y, Kataoka K, Takeuchi J, et al. Vascular maturity of type 1 and type 2 choroidal neovascularization evaluated by optical coherence tomography angiography. *PLoS One*. 2019;14(4):e0216304.
 17. Hikichi T, Agarie M, Kubo N, Yamauchi M. Predictors of recurrent exudation in choroidal neovascularization in age-related macular degeneration during a treatment-free period. *Retina*. 2020;40(11):2158–2165.
 18. Miere A, Butori P, Cohen SY, et al. Vascular remodeling of choroidal neovascularization after anti-vascular endothelial growth factor therapy visualized on optical coherence tomography angiography. *Retina*. 2019;39(3):548–557.
 19. Faatz H, Farecki ML, Rothaus K, et al. Changes in the OCT angiographic appearance of type 1 and type 2 CNV in exudative AMD during anti-VEGF treatment. *BMJ Open Ophthalmol*. 2019;4(1):e000369.
 20. Bae K, Kim HJ, Shin YK, Kang SW. Predictors of neovascular activity during neovascular age-related macular degeneration treatment based on optical coherence tomography angiography. *Sci Rep*. 2019;9(1):19240.
 21. Ciulla TA, Hussain RM, Pollack JS, Williams DF. Visual acuity outcomes and anti-vascular endothelial growth factor therapy intensity in neovascular age-related macular degeneration patients: a real-world analysis of 49 485 eyes. *Ophthalmol Retina*. 2020;4(1):19–30.
 22. Kido A, Miyake M, Tamura H, et al. Incidence and clinical practice of exudative age-related macular degeneration: a nationwide population-based cohort study. *Ophthalmol Sci*. 2022;2(2):100125.
 23. Arrigo A, Aragona E, Bianco L, et al. The localization of intraretinal cysts has a clinical role on the 2-year outcome of neovascular age-related macular degeneration. *Ophthalmol Retina*. 2023;7(12):1069–1079.
 24. Arrigo A, Aragona E, Battaglia Parodi M, Bandello F. Quantitative approaches in multimodal fundus imaging: state of the art and future perspectives. *Prog Retin Eye Res*. 2023;92:101111.